COMPARING CONSERVED CHARGE FLUCTUATIONS FROM LATTICE QCD TO HRG MODEL CALCULATIONS*

Jishnu Goswami, Frithjof Karsch, Christian Schmidt

Fakultät für Physik, Universität Bielefeld, 33615 Bielefeld, Germany

Swagato Mukherjee, Peter Petreczky

Physics Department, Brookhaven National Laboratory, Upton, NY 11973, USA

(Received November 25, 2020)

We present results from lattice QCD calculations for 2^{nd} and 4^{th} order cumulants of conserved charge fluctuations and correlations, and compare these with various High Resonance Gas (HRG) model calculations. We show that differences between HRG and QCD calculations already show up in the second order cumulants close to the pseudo-critical temperature for the chiral transition in $(2+1)$-flavor QCD and quickly grow large at higher temperatures. We also show that QCD results for strangeness fluctuations are enhanced over HRG model calculations which are based only on particles listed in the Particle Data Group tables as 3-star resonances. This suggests the importance of contributions from additional strange hadron resonances. We furthermore argue that additional (repulsive) interactions, introduced either through excluded volume (mean field) HRG models or the S-matrix approach, do not improve the quantitative agreement with 2^{nd} and 4^{th} order cumulants calculated in lattice QCD. HRG-based approaches fail to describe the thermodynamics of strongly interacting matter at or shortly above the pseudo-critical temperature of QCD.

DOI:10.5506/APhysPolBSupp.14.251

1. Introduction

The theory of strong interactions, Quantum Chromodynamics (QCD), also describes the thermodynamics of strongly interacting matter at finite temperature and density. It now is understood that at vanishing net-baryon-number density, the transition from low to high temperature reflects the physics of a true phase transition that occurs at vanishing values of the two

* Presented by J. Goswami at the on-line meeting *Criticality in QCD and the Hadron Resonance Gas*, Wrocław, Poland, July 29–31, 2020.

light (up and down)-quark masses in QCD, and is due to the restoration of chiral symmetry, which is spontaneously broken in the QCD vacuum and at low temperatures [1]. QCD with its physical spectrum of light and strange quark masses undergoes a smooth transition from hadronic bound states to the quark–gluon plasma (QGP) at high temperature.

Hadron Resonance Gas (HRG) models can be used to describe the thermodynamics of QCD at low temperature where the degrees of freedom of QCD matter are hadrons. This model assumes that interactions among hadrons can be accounted for by production of hadronic resonances which are added to thermodynamics as additional particles. The simplest implementation of a non-interacting HRG model considers a mixture of ideal Bose gases for mesons and ideal Fermi gases for baryons. The total pressure of a hadronic medium is then obtained as the sum over individual contributions of partial pressures of different particle species. The HRG model can be justified using the S-matrix-based virial expansion [2]. It has been shown that using partial wave analysis of the experimental scattering data, non-resonant repulsive and attractive interactions of hadrons largely cancel out in the thermodynamic quantities, and thus, the interactions can be indeed well-described by hadronic resonances [3]. This approach has been recently revisited in several papers [4–6], where also some of the non-resonant (repulsive) interactions were included.

HRG models have been used to extract information on thermal conditions at the time of freeze-out of hadrons from a high temperature partonic medium from experimental data on hadron yields [7]. However, a comparison of lattice QCD calculations of conserved charge fluctuations with corresponding HRG model calculations shows that the latter deviates from QCD results more and more with increasing temperature and deviations are larger for higher order cumulants. This short-coming of simple, non-interacting HRG models has been attempted to compensate by either taking into account further contributions from repulsive interactions through thermodynamic calculations with extended hadrons [8] or with a repulsive mean field [4], since a comprehensive treatment of the repulsive interactions in the S-matrix approach is not yet available. While these modifications of point-like, non-interacting HRG model calculations generically lead to a reduction of cumulants of conserved charge fluctuations, there is also evidence that strangeness fluctuations calculated in QCD are larger than those obtained in HRG model calculations based only on experimentally well-established (3-star resonances) hadrons listed by the Particle Data Group (PDG). One popular approach to address this issue is to include in HRG model calculations additional strange hadron resonances which are not listed in the PDG tables [9–11], but are obtained in quark model calculations [12, 13]. This may also be interpreted as an attempt to take care of further interactions.

We will present here a comparison of various cumulants of conserved charge fluctuations, calculated in $(2+1)$-flavor lattice QCD [9, 10], with different HRG model calculations. We mainly focus on the temperature range close to the transition temperature which is relevant for setting the baseline for heavy-ion collision experiments. In the following, we refer to the standard non-interacting HRG as PDG-HRG, where we consider down to 3-star hadrons and hadron resonances listed in PDG 2020 [14]. We also extended the HRG model based on resonances listed by the PDG by using additional hadronic resonances obtained in relativistic quark model calculations (QM-HRG [12, 13]). Furthermore, we discuss modifications of the non-interacting HRG models obtained by including further interactions between hadrons either through excluded volume or mean field effects (EV-HRG), or an advanced treatment of the S-matrix approach to the thermodynamics of strongly interacting hadrons.

2. Second order cumulants of conserved charge fluctuations and correlations

Here, we will discuss second order cumulants of net-baryon-number (B) and strangeness (S) fluctuations. In particular, we will compare the second order cumulants to various HRG model calculations and discuss to what extent deviations from HRG model results show up already on the level of these low order cumulants.

The pressure of the QCD partition function can be written as

$$\frac{P}{T^4} = \frac{1}{VT^3} \ln Z(V, T, \mu_B, \mu_Q, \mu_S)\,. \tag{1}$$

Generalized susceptibilities, *i.e.* the cumulants of conserved charge fluctuations, can be obtained by taking derivatives of the pressure with respect to baryon (μ_B), electric charge (μ_Q) and strangeness (μ_S) chemical potentials at $\vec{\mu} = (\mu_B, \mu_Q, \mu_S) = 0$

$$\chi^{BQS}_{lmn} = \left. \frac{\partial^{l+m+n} P/T^4}{\partial(\mu_B/T)^l \partial(\mu_Q/T)^m \partial(\mu_S/T)^n} \right|_{\vec{\mu}=0}\,. \tag{2}$$

2.1. Charge fluctuations

In Fig. 1 (left) and (middle), we show results for net-baryon-number (χ_2^B) and strangeness (χ_2^S) fluctuations (2^{nd} order cumulants). Results obtained on lattices of the size of $N_\sigma^3 \times N_\tau$, with $N_\sigma = 4N_\tau$ in $(2+1)$-flavor QCD simulations using the HISQ action [10, 15], are shown for several values of the lattice spacing, *i.e.* several values of temporal lattice extent $aN_\tau = 1/T$. These data have been extrapolated to the continuum limit using a quadratic Ansatz for discretization errors in (aT). As discussed above, we compare

these results to the HRG model calculations based on hadron spectra listed in the PDG and obtained in quark model calculations, respectively. Some basic formulas for the HRG model calculations are given in Appendices A and B.

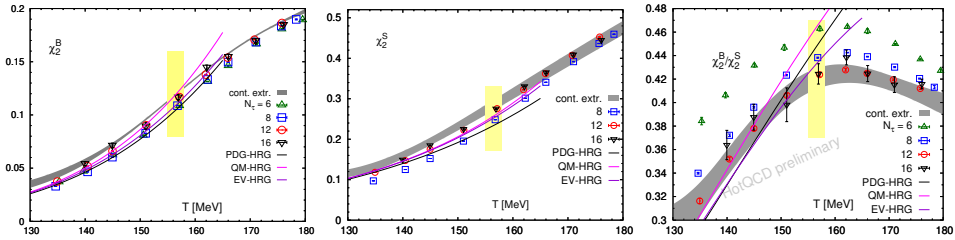

Fig. 1. Second order net-baryon-number (left) and strangeness (middle) fluctuations as well as their ratio (right).

It is quite evident for χ_2^B and χ_2^S that PDG-HRG curves provide only a poor description of the QCD results close to the transition region. The agreement of HRG model and QCD results improves when one includes additional strange-baryon resonances in the spectrum that are predicted in quark model calculations (QM-HRG). However, as can be seen clearly in Fig. 1 (right), the non-interacting HRG model calculations do not give a reasonable description of the QCD results at temperatures above the pseudo-critical temperature for the chiral transition, $T_{\rm pc} = (156.5 \pm 1.5)$ MeV [15]. In particular, HRG results for the χ_2^B/χ_2^S ratio continue to rise above $T_{\rm pc}$, while the QCD results have a maximum close to $T_{\rm pc}$ and then drop towards the non-interacting quark gas value, $(\chi_2^B/\chi_2^S)_{T\to\infty} = 1/3$. Similarly, it is apparent that temperature derivatives of the 2$^{\rm nd}$ order cumulants keep rising in the HRG model calculations, while they reach a maximum for the QCD results close to $T_{\rm pc}$.

At large temperatures, the HRG model results are significantly larger than the QCD results. This may, partly, be compensated by introducing repulsive interactions in the baryon sector of HRG. When using an excluded volume of the size of $b \simeq 0.4/T^3$, which corresponds to $rT \simeq 0.3$ or a hadron radius that varies in the range of (0.45–0.34) fm in the temperature range of (130–175) MeV that is of interest in our study[1], we find a reduction of χ_2^B of about 20% in the transition region. The influence on strangeness fluctuations is much smaller, *i.e.* about 8%, as these are dominated by mesons. We show results for the QM-HRG with excluded volume effects for baryons (EV-HRG) in Fig. 1. It is apparent that the hadronic interaction considered here is not sufficient to describe the QCD data. They rather tend to worsen the agreement between HRG and QCD calculations achieved by introducing additional strange-baryon resonances.

[1] Note that a constant radius $r \simeq 0.39$ fm has been used in [16, 17], which is close to our value of r in the pseudo-critical region.

2.2. Charge correlations and constraints on second order cumulants

In Fig. 2, we show QCD results for correlations among conserved charge fluctuations and compare with the HRG model calculations as discussed above for the 2nd order cumulants of conserved charge fluctuations. The general picture is the same. Additional strange-baryon resonances seem to be needed to improve agreement between the HRG model calculations for BS-correlations and corresponding QCD results, and the inclusion of repulsive interactions among baryons through excluded volume effects seems to deteriorate this agreement. Also shown in Fig. 2 is the result of an S-matrix calculation [5] that takes into account resonance decays in the $\Delta^{++} \leftrightarrow N^*\pi$ channel (see also Appendix C). As can also be seen, the S-matrix approach leads to a reduction of correlations between net-baryon-number and electric charge. The contribution of doubly charged Δ^{++} resonances seems thus to be suppressed.

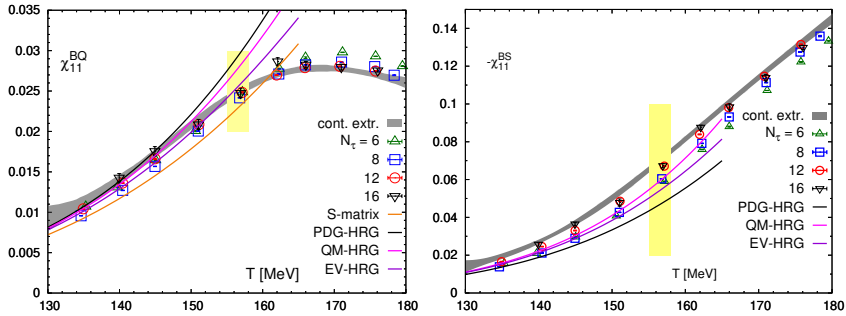

Fig. 2. Second order cumulants of net-baryon-number fluctuations correlated with net-electric charge (BQ) and strangeness (BS) fluctuations, respectively.

The three conserved charges (B, Q, S) give rise to the 6 second order cumulants of charge fluctuations and cross-correlations. In the isospin symmetric limit of degenerate up and down quark masses, which usually is used in lattice QCD calculations, only 4 of these cumulants are independent as isospin symmetry imposes the two constraints

$$\chi_2^S = 2\chi_{11}^{QS} - \chi_{11}^{BS}\,, \qquad \chi_2^B = 2\chi_{11}^{BQ} - \chi_{11}^{BS}\,. \tag{3}$$

This gives rise to three independent cumulant ratios, for instance, the set of three ratios of second order cumulants shown in Fig. 3. In Table I, we give results for continuum extrapolations of these three ratios at the pseudo-critical temperature, $T_{\rm pc} = 156.5(1.5)$ MeV, for the chiral transition in $(2+1)$-flavor QCD. Note, for instance, that due to the first constraint in Eq. (3), the χ_2^B/χ_2^S ratio shown in Fig. 1 (right) is related to the two ratios χ_{11}^{BS}/χ_2^S and χ_2^B/χ_{11}^{QS} shown in Fig. 3 and given in Table I at $T_{\rm pc}$

$$\frac{\chi_2^B}{\chi_2^S} = \frac{1}{2}\frac{\chi_2^B}{\chi_{11}^{QS}}\left(1 + \frac{\chi_{11}^{BS}}{\chi_2^S}\right), \tag{4}$$

and $(\chi_2^B/\chi_2^S)_{T_{\rm pc}} = 0.417(18)$.

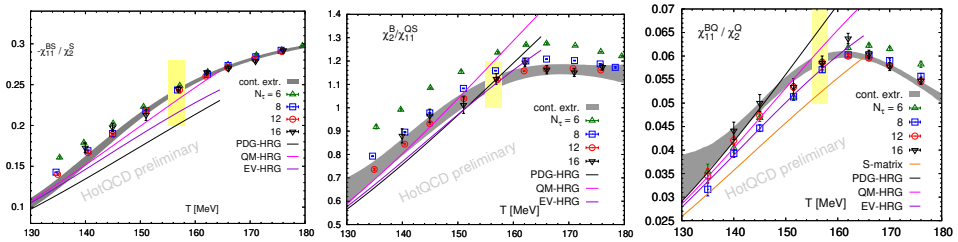

Fig. 3. Continuum extrapolated results for 2nd order cumulant ratios.

TABLE I

Continuum extrapolated results for three independent ratios of 2nd order cumulants at the pseudo-critical temperature $T_{\rm pc}$.

χ_{11}^{BS}/χ_2^S	χ_2^B/χ_{11}^{QS}	χ_{11}^{BQ}/χ_2^Q
−0.241(4)	1.10(4)	0.059(14)

3. Fourth order cumulants of conserved charge fluctuations and correlations

In a non-interacting HRG (PDG-HRG or QM-HRG), ratios of cumulants involving net-baryon-number fluctuations that differ only by an even number of derivatives with respect to the baryon chemical potential are unity, *e.g.* for fourth order cumulants $\chi_4^B/\chi_2^B = \chi_{31}^{BS}/\chi_{11}^{BS} = \chi_{31}^{BQ}/\chi_{11}^{BQ} = 1$. This reflects that all known hadrons with non-zero baryon number have $|B| = 1$. This, of course, does not hold in QCD at high temperatures where quarks carry non-integer baryon number. As a consequence, the above ratios are all found to be smaller than unity in lattice QCD calculations. They are shown in Fig. 4.

At low temperatures, the deviations from unity follow a trend also present in HRG model calculations that incorporates excluded volume effects. This is also shown in Fig. 4. Although the agreement of these model calculations with lattice QCD data seems to be reasonable below the pseudo-critical temperature, we note that this is to some extent accidental as the EV-HRG calculations do not provide an adequate description for neither the numerator nor the denominator of these ratios. *E.g.*, in the case of quadratic (χ_2^B)

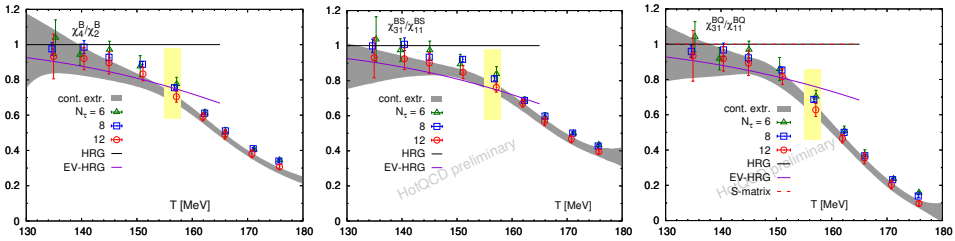

Fig. 4. Ratios of some fourth and second order cumulants.

and quartic (χ_4^B) net-baryon-number fluctuations, the EV-HRG calculations both underestimate the QCD results. We also note that in the present implementation of the S-matrix approach, the $\chi_{31}^{BQ}/\chi_{11}^{BQ}$ ratio remains unity like it is the case in non-interacting HRG models.

4. Conclusions

Qualitative features of 2$^{\rm nd}$ and 4$^{\rm th}$ order cumulants of conserved charge fluctuations and correlations, calculated in lattice QCD, are reasonably well-described by non-interacting HRG models up to the pseudo-critical temperature for the QCD transition. At higher temperatures, significant deviations quickly set in, being large already for temperatures about 10% higher than $T_{\rm pc}$ and being larger for 4$^{\rm th}$ than for 2$^{\rm nd}$ order cumulants. In order to reach a somewhat satisfactory description of strangeness fluctuations, the addition of strange resonances calculated in quark models (QM-HRG model) is needed, which may be viewed as taking care of additional interactions, represented for instance in less well-established resonances listed in the PDG, which are not reflected in HRG models based on down to 3-star resonances only. Including further interactions through *e.g.* excluded volume, HRG models (EV-HRG) or S-matrix approaches do not seem to lead to a further quantitative improvement of many of the cumulants considered here.

This work was supported by the TU Deutsche Forschungsgemeinschaft (DFG) — project No. 315477589-TRR 211, the European Union H2020-MSCA-ITN-2018-813942 (EuroPLEx), and the U.S. Department of Energy, Office of Science, Office of Nuclear Physics through *(i)* the Contract No. DE-SC 0012704, *(ii)* within the framework of the Beam Energy Scan Theory (BEST) Topical Collaboration, and *(iii)* the Office of Nuclear Physics and Office of Advanced Scientific Computing Research within the framework of Scientific Discovery through Advance Computing (SciDAC) award "Computing the Properties of Matter with Leadership Computing Resources".

Appendix A

Non-interacting HRG Model

The pressure of a non-interacting hadron gas can be written as a sum of contributions for mesons (M) and baryons (B) and the corresponding anti-particles ($\bar{M}$, $\bar{B}$)

$$P = P_M + P_{\bar{M}} + P_B + P_{\bar{B}}\,, \tag{A.1}$$

$$\frac{P}{T^4} = \sum_{H\in B,\bar{B}} \frac{g}{2\pi^2}\left(\frac{m_H}{T}\right)^2 \sum_{k=1}^{\infty} \frac{(-1)^{k+1}}{k^2} K_2\left(\frac{km_H}{T}\right) \exp\left[k\vec{C}_H.\vec{\mu}/T\right] + \sum_{H\in M,\bar{M}} \frac{g}{2\pi^2}\left(\frac{m_H}{T}\right)^2 \sum_{k=1}^{\infty} \frac{1}{k^2} K_2\left(\frac{km_H}{T}\right) \exp\left[k\vec{C}_H.\vec{\mu}/T\right]\,, \tag{A.2}$$

where $\vec{C}_H = (B_H, Q_H, S_H)$ represents the conserved charges, *i.e.* baryon number, electric charge and strangeness number of the hadron H, and μ_B, μ_Q, μ_S are the baryon, electric charge and strangeness chemical potentials, respectively. K_2 is the modified Bessel function of the second kind. Generalized susceptibility can be obtained from Eq. (2)

$$\chi^{BQS}_{lmn} = \sum_{H\in B,\bar{B}} \frac{g_H}{2\pi^2}\left(\frac{m_H}{T}\right)^2 B_H^l Q_H^m S_H^n\; K_2\left(\frac{m_H}{T}\right) + \sum_{H\in M,\bar{M}} \frac{g_H}{2\pi^2}\left(\frac{m_H}{T}\right)^2 \sum_{k=1}^{\infty} (kQ_H)^m (kS_H)^n \frac{1}{k^2} K_2\left(\frac{km_H}{T}\right). \tag{A.3}$$

In Eq. (A.3), the first term corresponds to the baryon sector, where we only used the Boltzmann approximation to the Fermi sum given in Eq. (A.2), and the second term corresponds to the meson sector. Note that the second term will drop out from Eq. (A.3) for any baryonic observables as baryon number (B) is 0 for mesons.

Appendix B

Excluded volume HRG model

In excluded volume, we only consider the interaction between baryons, BB, and anti-baryons, $\bar{B}\bar{B}$. The meson–meson, MM, and meson–baryon, $MB(\bar{B})$, as well as baryon–anti-baryon, $B\bar{B}$, interactions are neglected. Hence, the excluded volume will only modify P_B and $P_{\bar{B}}$ independently, and the total pressure Eq. (A.1) can be replaced by

$$P = P_M + P_{\bar{M}} + P_B^{\rm int} + P_{\bar{B}}^{\rm int}\,, \tag{B.1}$$

where the interacting baryon or anti-baryon pressure can be written as

$$\hat{P}^{\rm int}_{B/\bar{B}} \;=\; \sum_{H\in B/\bar{B}} \hat{P}^{\rm id}_{H}(T,\vec{\mu}\,)\;\exp\left[-b'\hat{P}^{\rm int}_{B/\bar{B}}\right]\,, \tag{B.2}$$

with $b' = bT^3$, $P = P/T^4$ and $\hat{P}^{\rm id}_{H}(T,\vec{\mu})$ denoting the ideal gas pressure for baryon species H with mass m_H. This equation may be solved iteratively

$$\begin{aligned}\hat{P}^{\rm int}_{B/\bar{B}} \;=\; &\sum_{H\in B/\bar{B}} \hat{P}^{\rm id}_{H}(T,\vec{\mu}\,) - b'\left[\sum_{H,H'\in B/\bar{B}} \hat{P}^{\rm id}_{nm}(T,\vec{\mu}\,)\right]^2 \\ &+ \left(3b'^2/2\right)\left[\sum_{H,H',H''\in B/\bar{B}} \hat{P}^{\rm id}_{lmn}(T,\vec{\mu})\right]^3 + \ldots\end{aligned} \tag{B.3}$$

For the baryon species H, $\hat{P}^{\rm id}_{H}(T,\vec{\mu}\,)$ can be written from Eq. (A.2) using the Boltzmann approximation as

$$\hat{P}^{\rm id}_{H} \;=\; \frac{g_H}{2\pi^2}(m_H/T)^2 K_2\left(\frac{m_H}{T}\right)\exp\left[\vec{C}_H.\vec{\mu}/T\right]\,. \tag{B.4}$$

The term linear in b' appearing in Eq. (B.4) acts as a repulsive term. It decreases the pressure and is related to the second virial coefficient. The term quadratic in b acts as an attractive term. However, since $\hat{P}^{\rm id}_{H} \sim \exp(-m_H/T)$, only the term linear in b will survive for $m_H \gg T$ at high temperature, *i.e.* excluded volume effects are predominantly repulsive. Moreover, since for low temperatures $\hat{P}^{\rm id}_{H} \to 0$, $\hat{P}^{\rm int}_{H}$ will also approach $\hat{P}^{\rm id}_{H}$.

Generalized susceptibilities can be obtained by taking derivatives of Eq. (B.2) with respect to chemical potentials (μ_B, μ_Q and μ_S). We also note that the resulting equations in the mean field approach [4] are quite similar to those obtained in the excluded volume approach. The difference is that in mean field approach the repulsive interactions have been used only for the baryon octet and decuplet, while in the excluded volume approach, one generally considers interaction between all baryons.

Appendix C

S-matrix formalism

In the S-matrix formalism as used here by us, we only considered the decay and production of $N^*$and Δ^{++} to pion and nucleon in a hot hadron gas. The pressure can then be separated into two parts; one part arises from the interaction of pion and nucleon, the other part describes the contribution from all other particles

$$\hat{P} \;=\; \hat{P}^{\rm id} + \sum_{I_z=3/2,1/2} \hat{P}^{\rm int}\,, \tag{C.1}$$

$$\hat{P}^{\rm int} \;=\; \frac{g}{2\pi^2} \int\limits_{m_{\rm th}}^{\infty} {\rm d}\epsilon\; K_2(\epsilon/T)\; (\epsilon/T)^2\; \frac{{\rm d}\delta_{IJ}}{\pi {\rm d}\epsilon}\,, \tag{C.2}$$

where $\hat{P}^{\rm id}$ is the same as in Eq. (A.2), but without the contribution from Δ^{++} and N^* resonances. Their contribution to the pressure is included in the $\hat{P}^{\rm int}$. Here, we follow the notation and steps of [3, 5] for calculating the cumulants of net-baryon-number and electric charge correlations, χ^{BQ}_{nm}, in the S-matrix approach.

REFERENCES

[1] For a recent review see: O. Philipsen, *PoS* **LATTICE2019**, 273 (2019), arXiv:1912.04827 [hep-lat]; H.-T. Ding, F. Karsch, S. Mukherjee, *Int. J. Mod. Phys. E* **24**, 1530007 (2015), arXiv:1504.05274 [hep-lat].

[2] R. Dashen, S.k. Ma, H.J. Bernstein, *Phys. Rev.* **187**, 345 (1969).

[3] R. Venugopalan, M. Prakash, *Nucl. Phys. A* **546**, 718 (1992).

[4] P. Huovinen, P. Petreczky, *Phys. Lett. B* **777**, 125 (2018), arXiv:1708.00879 [hep-ph].

[5] P.M. Lo *et al.*, *Phys. Lett. B* **778**, 454 (2018), arXiv:1710.02711 [hep-ph].

[6] C. Fernández-Ramírez, P.M. Lo, P. Petreczky, *Phys. Rev. C* **98**, 044910 (2018), arXiv:1806.02177 [hep-ph].

[7] J. Stachel *et al.*, *J. Phys.: Conf. Ser.* **509**, 012019 (2014), arXiv:1311.4662 [nucl-th].

[8] G.D. Yen *et al.*, *Phys. Rev. C* **56**, 2210 (1997), arXiv:nucl-th/9711062.

[9] A. Bazavov *et al.*, *Phys. Rev. Lett.* **113**, 072001 (2014), arXiv:1404.6511 [hep-lat].

[10] A. Bazavov *et al.*, *Phys. Rev. D* **95**, 054504 (2017), arXiv:1701.04325 [hep-lat].

[11] A. Pásztor *et al.*, *EPJ Web Conf.* **175**, 07046 (2018).

[12] S. Capstick, N. Isgur, *Phys. Rev. D* **34**, 2809 (1986).

[13] D. Ebert, R.N. Faustov, V.O. Galkin, *Phys. Rev. D* **79**, 114029 (2009), arXiv:0903.5183 [hep-ph].

[14] Particle Data Group (P.A. Zyla *et al.*), *Prog. Theor. Exp. Phys.* **2020**, 083C01 (2020).

[15] HotQCD Collaboration (A. Bazavov *et al.*), *Phys. Lett. B* **795**, 15 (2019), arXiv:1812.08235 [hep-lat].

[16] V. Vovchenko *et al.*, *Phys. Rev. Lett.* **118**, 182301 (2017), arXiv:1609.03975 [hep-ph].

[17] V. Vovchenko, *et al.*, *Phys. Lett. B* **775**, 71 (2017), arXiv:1708.02852 [hep-ph].